

Bozhou WANG, Weipeng LAI, Qian LIU, Peng LIAN,
Yongqiang XUE

Synthesis, characterization and quantum chemistry study of 3,6-bis(1H-1,2,3,4-tetrazol-5-yl-amino)-1,2,4,5-tetrazine

© Higher Education Press and Springer-Verlag 2009

Abstract 3,6-bis(1H-1,2,3,4-tetrazol-5-yl-amino)-1,2,4,5-tetrazine (BTATz) was synthesized by the condensation of triaminoguanidinium nitrate with 2,4-pentanedione, followed by oxidation and substitution reaction. The product was characterized by elemental analysis, IR, NMR spectrometry and DSC analysis. Instead of nitrogen dioxide/N-methylpyrrolidone, acetic acid/sodium nitrite was used as the oxidizer during the oxidation. Thus, the cost was reduced and the process was simplified. The theoretical properties of BTATz were estimated by a B3LYP method based on a 6-31G(d,p) basis set, and the stable geometric configuration and bond order were obtained. The vibrational frequencies, IR spectrum and thermodynamic properties under different temperatures were obtained from vibrational analysis and the relationship between temperature and thermodynamics properties was deduced. Pyrolysis mechanism of BTATz was discussed and the transition state and activation energy of ring opening reaction of the tetrazole were deduced.

Keywords 3,6-bis(1H-1,2,3,4-tetrazol-5-yl-amino)-1,2,4,5-tetrazine (BTATz), synthesis, theoretical calculation, geometric configuration, thermodynamics property, pyrolysis mechanism

Nitrogen-rich energetic compounds have a lot of N–N and C–N bonds. These kinds of energetic compounds have high nitrogen content, high positive enthalpy, big explosive heat and strong power [1]. When nitrogen-rich energetic compounds are decomposed, a lot of nitrogen and

enormous energy are produced. This kind of compound is widely applied in the field of energetic materials, such as insensitive high explosives, low signal propellants, gas-forming agents and pyrotechnics. At present, Nitrogen-rich energetic compounds have been a hotspot in energetic materials worldwide.

3,6-Bis(1H-1,2,3,4-tetrazol-5-yl-amino)-1,2,4,5-tetrazine (BTATz) was firstly synthesized by Hiskey in Los Alamos National Laboratory [2,3]. Because its nitrogen content reached 80%, the thermal and chemical stability are relatively good, the velocity of inflammation is high, the pressure exponent and sensitivity are relatively low. BTATz has drawn a great deal of attention worldwide. At present, the synthesis and combustion property of BTATz have been researched by scientists all over the world [4–7]. However, the quantum chemistry of BTATz has not been reported in the literature.

In this paper, BTATz was synthesized by condensation of triaminoguanidinium nitrate with 2,4-pentanedione, followed by oxidation and substitution reaction (Scheme 1). The synthetic method of BTATz was investigated and its oxidation process was improved in order to simplify the operation and to reduce the synthetic cost. The geometry configuration, bond order, vibration, infrared spectrum, thermodynamic property and pyrolysis mechanism were studied by quantum chemistry calculation.

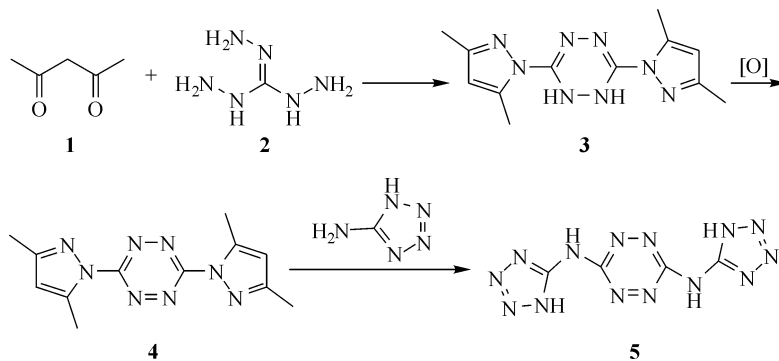
1 Experiments

The following instruments were used: PE-2400 Type Elemental Analysis Instrument, NEXUS870 Type Fourier Transform IR Sepctrum Instrument, AV500 Typeo (500 MHz) Superconductive NMR Instrument, DSC-60 Type DSC Instrument.

Triaminoguanidinium nitrate and 5-aminotetrazole (5-AT) were prepared in this lab. 2,4-Pentanedione, sodium nitrite, N-methylpyrrolidone, sulfolane, acetic acid, 30%

Translated from *Chinese Journal of Organic Chemistry*, 2008, 28(3) (in Chinese)

Bozhou WANG (✉), Weipeng LAI, Qian LIU, Peng LIAN,
Yongqiang XUE
Xi'an Modern Chemistry Research Institute, Xi'an 710065, China
E-mail: wbz600@163.com



Scheme 1

hydrogen peroxide, ethanol, dimethylformamide (DMF) and other reagents are at C.P. levels.

1.1 Synthesis of 3,6-bis(3,5-dimethylpyrazole-1-yl)-1,2-dihydro-1,2,4,5-tetrazine (3)

2,4-Pentanedione (40 g, 0.4 mol) was dropwise added to the water solution of triaminoguanidinium nitrate (33.4 g, 0.2 mol), the temperature was increased to 70°C and the reaction was continued for 2 h. After the reaction solution was cooled to room temperature, a lot of solids were separated out, filtrated and washed by cooled water and then dried. An orange yellow solid **3** (44 g) was obtained with a yield of 80%, m.p. 149–151°C; ¹H NMR (CD₃Cl, 500 MHz) δ: 8.09 (s, 2H, NH), 5.97 (s, 2H, CH), 2.49 (s, 6H, NCCH₃), 2.23 (s, 6H, N=CCH₃); ¹³C NMR (CD₃Cl, 500 MHz) δ: 150.01, 145.88, 142.39, 109.92, 13.84, 13.52; IR (KBr) ν: 3250, 1568, 1473, 1414, 967 cm⁻¹.

1.2 Synthesis of 3,6-bis(3,5-dimethylpyrazole-1-yl)-1,2,4,5-tetrazine (4)

Sulfolane (60.0 g, 0.22 mol), compound **3** and 450 mL acetic acid were mixed and stirred. The temperature was increased to 40°C. 15.5 g sodium nitrite was added in batches and the reaction was continued for 2 h. The reaction solution was cooled and poured into a mass of cool water. A lot of solid was separated out, filtrated, washed by cooled water and dried. A red solid **4** (52.6 g) was obtained with a yield of 88%. m.p. 225–227°C; ¹H NMR (CD₃Cl, 500 MHz) δ: 6.19 (s, 2H, CH), 2.76 (s, 6H, NCCH₃), 2.43 (s, 6H, N=CCH₃); IR (KBr) ν: 1578, 1484, 1425, 970 cm⁻¹. Anal. Calcd. for C₁₂H₁₄N₈: N 41.48, C 53.33, H 5.19; found N 41.18, C 53.43, H 4.85.

1.3 Synthesis of BTATz (5)

Sulfolane (400 mL), compound **4** (40 g, 0.147 mol) and 5-AT (32 g, 0.340 mol) were mixed and stirred. The temperature was slowly increased to 135°C and maintained for 18 h. After the reaction solution was cooled to 50°C, 40 mL DMF was added, a lot of solid was separated out,

filtrated, washed by DMF, and dried for 3 d at 100°C, giving 33 g russet solid. The crude product was treated with 400 mL DMF, 14.8 g of orange yellow solid **5** was obtained with a yield of 40%.

¹H NMR (DMSO-d₆, 500 MHz) δ: 12.5 (s, 2H, NH); IR (KBr) ν: 3428, 3336, 1615, 1491, 1443, 1067 cm⁻¹; Anal. calcd. for C₄H₄N₁₄: N 79.02, C 19.36, H 1.62; found N 78.90, C 19.51, H 1.78; DSC (10 min/°C) T_m: 317.12 °C.

1.4 Computational method and principle

Because the B3LYP method is considered to have adequate electronic relevance, maintained many merits of ab initio and saved a lot of computational time, it has obtained widespread applications [8–14]. The calculation results by this method are good, for tetrazole compounds [15,16]. The molecular structure and the performance given under 6-31G(d, p) level also approached the experimental value. Therefore, following the Gaussian98 second edition of application procedure DFT-B3LYP/6-31G(d, p) method, all computations were obtained.

2 Results and discussion

2.1 Experimental part

2.1.1 Oxidation reaction

Compound **4** is an important energetic intermediate to synthesize many kinds of tetrazine-based nitrogen-rich energetic compounds. In this paper, preparation of compound **4** by the oxidation of compound **3** was improved. It was reported [3] that with N-methylpyrrolidone (NMP) as the reaction medium and NO₂ as the oxidizer, compound **4** was prepared in a yield over 90%. However, this method had some limitations, such as the use of costly reagent NMP and the difficulty for the preparation of NO₂. In our research, air, 30% hydrogen peroxide and sodium nitrite/acetic acid were used as the oxidizer instead of nitrogen dioxide for the synthesis of compound **4**, and the experimental results are shown in Table 1.

Table 1 Comparison of the synthesis of **4** from different oxidizers

Oxidizer	Medium	Time	m.p./ °C	Yield/%
NO ₂	NMP	1 h	225–227	90
Air	NMP	> 14 d	220–225	10
H ₂ O ₂	NMP	>	222–226	15
NaNO ₂	acetic acid	2 h	225–227	85

It was found from Table 1 that with air or 30% hydrogen peroxide as the oxidizer, the reaction time was longer and the yield was lower. The product was very difficult to purify. However, with cheap sodium nitrite/acetic acid as the oxidizer, the reaction has a relatively high yield and thus, possesses potential applications in the future.

2.1.2 Substitution reaction

Two main products were obtained, respectively, at different temperatures by the substitution reaction of **4** with 5-aminotetrazole(5-AT) as shown in Scheme 2.

When the reaction temperature was 120°C, a mono substitution was produced by the substitution reaction of one molecule **4** with one molecule 5-AT. When the reaction temperature was increased to 135°C, the substitution reaction may be complete and the target compound **5** was obtained. Thus, the reaction temperature must be over 135°C in order to reduce the amount of by-products.

2.2 Quantum chemistry computation part

2.2.1 Geometry configuration

The geometry of BTATz was optimized, and the configuration and the atomic serial number of BTATz are listed in Fig. 1. The bond length, the bond angle and the dihedral angle data were shown in Table 2 (Because the structure of BTATz had high central symmetry, Table 2 only lists the single-side data of the symmetry center). The calculated vibrational frequencies were positive in value. The obtained configuration corresponded to the minimum point of the potential energy surface and was a relatively steady structure.

It was found from Fig. 1 and Table 2 that all the atoms of BTATz were nearly in a plane. The five-atom ring and six-atom ring respectively formed a conjugated system. In the five-atom ring, the N atom connected with the H atom

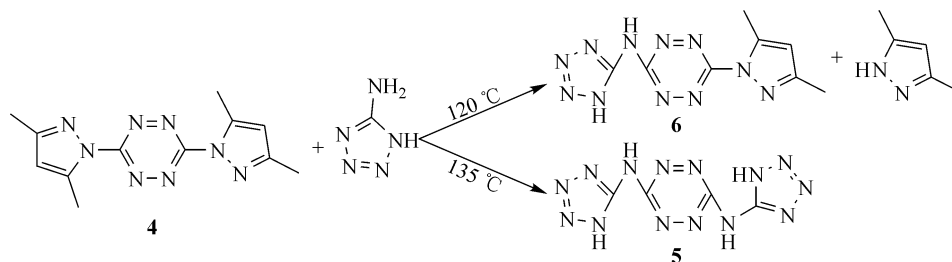
could provide a pair of electrons. Each of the other four atoms provided one electron to satisfy the $4n + 2$ aromatic rule. In the six-atom ring, each of the six atoms provided one electron to satisfy the $4n + 2$ aromatic rule. The five-atom ring and six-atom ring provided six electrons, respectively. Two N atoms linked with the three rings provided two electrons, respectively, and thus the entire molecular system could provide 22 electrons in all to satisfy the $4n + 2$ aromatic rule, forming a big conjugated system. Owing to the formation of the conjugated system, the bond length of N-N and C-N on the rings were in scopes of 1.289–1.378 Å, which were longer than the standard double bond (1.22 Å) and shorter than the standard single bond (1.46 Å). Because the bond length tended to an average, it enabled the entire molecule to have a good aromaticity and stability.

2.2.2 Bond order

Bond order played a very important role to judge a strong or weak bond in a molecule. After geometry optimization at B3LYP/6-31G(d, p) level, the bond orders of BTATz and natural bond orbital analysis (NBO) are shown in Table 3 (only a single-side data of the symmetry center). It was obvious from Table 3 that the bond orders of atoms on tetrazine ring were big, so that the tetrazine ring was not easy to break. The bond orders of N(14)-N(15) and N(18)-N(20) on the tetrazole rings were smaller, indicating that these bonds were easy to break causing the split of the tetrazole ring. Moreover, the orders of C-N bond connecting the tetrazole rings and the tetrazine ring were also small, making separation of the rings easy.

2.2.3 Vibration and infrared spectrum

The computed vibrational frequencies and intensities of BTATz (correction factor was 0.9613) are listed in Table 4. In Table 4, BTATz mainly had several strong absorptive peaks, such as 3495.62 cm⁻¹ and 3480.52 cm⁻¹. The 3495.62 cm⁻¹ absorptive peak corresponded to the stretching vibrations of N-H bonds in the tetrazole rings, while the peak at 3480.52 cm⁻¹ corresponded to that of N-H bonds between the tetrazole ring and the tetrazine ring. The peak at 1587.50 cm⁻¹ corresponded to the stretching vibrations of C(11)-N(3) and C(17)-N(5) and their related

**Scheme 2**

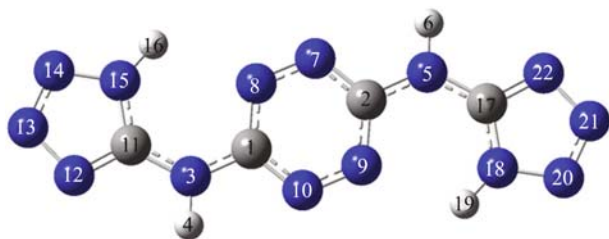


Fig. 1 The geometric configuration of BTATz after optimization at B3LYP/6-31G(d,p) level

ring's bending vibrations. The peak at 1503.38 cm^{-1} corresponded to the stretching vibrations of C(11)-N(15) and C(17)-N(18) on the tetrazole rings, and the one at 1429.95 cm^{-1} corresponded to the stretching vibrations of C(1)-N(3) and C(2)-N(5) and their related bending vibrations of the tetrazole rings. The peak at 1391.90 cm^{-1} related to the stretching vibrations of N-N on the tetrazine ring and their related ring's bending vibrations, while the one at 1029.84 cm^{-1} related to the in-plane bending vibrations of the tetrazine ring.

Comparison of the computation frequency with the experiment frequency clearly revealed that both data were very consistent, although there were still some deviations because of some solvent effect in the tests.

2.2.4 Thermodynamic property

BTATz structure was optimized by B3LYP/6-31G(d,p), and the standard thermodynamics function values in 273–1000 K temperature range are shown in Table 5. It was found from Table 5 that all the thermodynamics function values increased with the increment of temperature from 273 to 1000 K. The functions of the heat energy ($E_{t,m}^\theta$), the heat capacity ($C_{p,m}^\theta$), the entropy (S_m^θ) and the temperature (T) in the 273–1000 K temperature range were as follows:

$$E_{t,m}^\theta = 0.0002T^2 + 0.1473T + 346.65$$

$$C_{p,m}^\theta = -0.0004T^2 + 0.7992T + 12.971$$

$$S_{p,m}^\theta = -0.0002T^2 + 0.8578T + 263.04$$

The corresponding correlation coefficients were 0.9999, 0.9996 and 1, respectively. Moreover, a formula of $dC_{p,m}^\theta/dT = 0.7992 - 0.0008T$ was also obtained, indicating that in the 273–1000 K range, when the temperature was higher, the change of $C_{p,m}^\theta$ was becoming more and more slow. In the condition of $T > 999\text{ K}$ and $dC_{p,m}^\theta/dT < 0$, $C_{p,m}^\theta$ would decrease with the increment of temperature. It was helpful for further study of the detonation properties and other thermodynamic properties of BTATz via the above-mentioned calculated thermodynamic functions.

Table 2 The geometric parameters of BTATz after optimization at B3LYP/6-31G(d,p) level

Bond length/ Å		Bond angle/(°)		Dihedral angle/(°)	
C(1)-N(3)	1.368	C(1)-N(3)-H(4)	116.850	C(2)-C(1)-N(3)-H(4)	0.023
N(3)-H(4)	1.012	C(2)-N(7)-N(8)	117.419	N(3)-C(1)-C(2)-N(5)	179.967
C(1)-N(8)	1.351	C(1)-N(8)-N(7)	117.713	N(3)-C(1)-C(2)-N(7)	179.976
C(1)-N(10)	1.348	C(1)-N(3)-C(11)	127.435	C(1)-C(2)-N(7)-N(8)	0.000
N(7)-N(8)	1.311	N(8)-C(1)-N(10)	124.869	N(8)-C(1)-C(2)-N(9)	-180.000
N(3)-C(11)	1.378	N(3)-C(11)-N(12)	123.631	N(10)-C(1)-N(3)-C(11)	180.000
C(11)-N(12)	1.320	C(11)-N(12)-N(13)	105.120	C(2)-C(1)-N(3)-C(11)	-179.980
N(12)-N(13)	1.362	N(12)-N(13)-N(14)	111.809	C(1)-N(3)-C(11)-N(12)	-179.997
N(13)-N(14)	1.289	C(11)-N(15)-H(16)	128.441	C(1)-N(3)-C(11)-N(15)	0.000
N(14)-N(15)	1.362	C(11)-N(15)-N(14)	107.757	N(3)-C(11)-N(15)-H(16)	0.000
C(11)-N(15)	1.346	N(15)-N(14)-N(13)	106.096		
N(15)-H(16)	1.012				

Table 3 The bond order of BTATz at B3LYP/6-31G(d,p) level

Bond	Bond Order	Bond	Bond Order	Bond	Bond Order
C(1)-N(3)	0.9580	C(1)-N(8)	1.0939	N(9)-N(10)	1.0379
N(3)-H(4)	0.6608	N(3)-C(11)	0.9284	N(12)-C(11)	1.1734
C(1)-N(10)	1.1050	C(11)-N(15)	1.0227	N(12)-N(13)	0.9585
N(13)-N(14)	1.1583	N(14)-N(15)	0.8841	N(15)-H(16)	0.6701

Table 4 The vibrational frequencies (cm^{-1}) and intensities ($\text{kJ}\cdot\text{mol}^{-1}$) of BTATz at B3LYP/6-31G (d,p) level

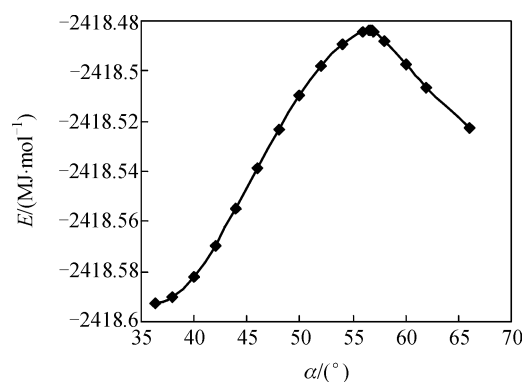
v1	792.47 (0.00)	v2	864.82 (13.23)	v3	872.95 (0.00)
v4	977.89 (0.49)	v5	978.24 (0.00)	v6	984.79 (174.21)
v7	985.87 (0.00)	v8	1009.13 (42.67)	v9	1029.84 (155.27)
v10	1043.13 (0.00)	v11	1047.15 (57.46)	v12	1089.87 (0.00)
v13	1095.88 (4.51)	v14	1211.10 (25.90)	v15	1215.77 (0.00)
v16	1244.39 (35.47)	v17	1255.88 (0.00)	v18	1319.02 (0.00)
v19	1320.32 (11.24)	v20	1385.12 (0.00)	v21	1391.90 (221.52)
v22	1429.95 (251.09)	v23	1459.93 (0.00)	v24	1480.90 (0.00)
v25	1503.38 (294.53)	v26	1520.58 (0.00)	v27	1587.50 (1924.96)
v28	1609.64 (0.00)	v29	3480.52 (236.73)	v30	3482.04 (0.10)
v31	3495.62 (217.50)	v32	3495.94 (2.00)		

Table 5 The thermodynamics properties of BTATz at different temperatures

T/K	$E_{tm}^{\theta}/(\text{kJ}\cdot\text{mol}^{-1})$	$C_{p,m}^{\theta}/(\text{J}\cdot\text{mol}^{-1}\cdot\text{K}^{-1})$	$S_m^{\theta}/(\text{J}\cdot\text{mol}^{-1}\cdot\text{K}^{-1})$
273	399.8185	201.4260	481.1177
298.15	404.8719	217.0134	499.5480
300	405.2571	218.1480	500.8920
400	429.1721	275.2434	571.6866
500	458.2913	321.9807	638.3321
600	491.5596	358.4226	700.4014
700	528.0350	386.5370	757.8569
800	566.9974	408.4297	810.9622
900	607.9066	425.7589	860.1069
1000	650.3733	439.7261	905.7137

2.2.5 Thermal decomposition mechanism

It was very important to study the thermal decomposition mechanism of the high energy density compound [17,18]. The computed bond orders of BTATz indicated that N(14)-N(15) was easy to break and caused the tetrazole ring split. Therefore, in this paper, the included angle α of N(15)-C(11)-N(14) was ruled as the reaction coordinate, the thermal decomposition process was described by the gradual increase of its value. The thermal decomposition potential curve was computed according to the reaction coordinate (see Fig. 2). The potential curve was drawn by connection of every single point energy which was calculated and obtained by a definite length along the reaction coordinate. In Fig. 2, it was found that when the α angle of N(15)-C(11)-N(14) increased gradually from 36.4° , the system energy gradually increased. When α was 56.6° , the system energy was reached to the maximum, then the system energy gradually decreased with α increase. The transition state (TS) was obtained by geometry optimization at the nearby curve peak and had only one frequency of negative value, the IRC analysis shows that the reactant and the product were connected by TS. Thermal decomposition activation energy E_a was $108.60 \text{ kJ}\cdot\text{mol}^{-1}$.

**Fig. 2** The thermo-decomposition potential curves of ring-opening of BTATz

3 Conclusion

Taking triaminoguanidinium nitrate and 2,4-pentanedione as the primary materials, 3,6-bis(1H-1,2,3,4-tetrazol-5-yl-amino)-1,2,4,5-tetrazine (BTATz) was synthesized by a three-step reaction. Its structure was characterized by elemental analysis, IR, NMR spectrometry and DSC analysis. It was found that instead of nitrogen dioxide/N-methylpyrrolidone, acetic acid/sodium nitrite was used as

the oxidizer. The cost was reduced and the process was simplified. All the atoms of BTATz were nearly in a plane. The tetrazine ring and tetrazole rings were connected via amino and the whole molecule could form a big conjugated system. The calculated bond orders of BTATz shows that the bond orders of atoms on the tetrazine ring were bigger, so it was not easy to break. The bond orders of N(14)-N(15) and N(18)-N(20) on the tetrazole rings were smaller, indicating that the tetrazole rings were easy to break. Because the C–N bond orders connecting the tetrazole rings and the tetrazine ring were also small, the two rings were separated easily. The obtained vibrations and infrared spectrum of BTATz indicated that the computation frequency and the experiment frequency tallied very well. Analysis of the relationship between thermodynamic property and temperature indicated that the heat energy ($E_{t,m}^{\theta}$), the heat capacity ($C_{p,m}^{\theta}$) and the entropy (S_m^{θ}) would increase with the temperature increase. The activation energy of breaking the tetrazole ring was $108.60 \text{ kJ} \cdot \text{mol}^{-1}$.

References

1. Hiskey M A, Nir G, James R S. High-nitrogen energetic materials derived from azotetrazolate. *J Energ Mater*, 1998, 16(2): 119–127
2. Hiskey M A, Chavez D, Naud D N. Progress in high-nitrogen chemistry in explosives, propellants and pyrotechnics. Proc.27th International Pyrotechnics Seminar, July 16–21, USA: Colorado, 2000: 3–14
3. Hiskey M A, Chavez D, Darrenl N. Propellant containing 3,6-bis(1H-1,2,3,4-tetrazol-5-yl-amino)-1,2,4,5-tetrazine or salts thereof. US 6 458 227, 2002. [Chem Abstr 2002, 137: 265190r]
4. Lu Y C. Proceedings of Halon Options Technical Working Conference, 2000, 316–370
5. Chavez D, Hiskey M A, Naud D N. Tetrazine explosives. *Propellants, Explos, Pyrotech*, 2004, 29(4): 209–215
6. Yue S T, Yang S Q. Synthesis and properties of 3, 6-bis(1H-1,2,3,4-tetrazol-5-yl-amino)-1,2,4,5-tetrazine. *Chin J Energ Mater*, 2004, 12(3): 155–157 (in Chinese)
7. Yue S T, Yang S Q. Synthesis and characterization of 3,6-bis(1H-1,2,3,4-tetrazol-5-yl-amino)-1,2,4,5-tetrazine. *Chin J Syn Chem*, 2004, 12(2): 164–166 (in Chinese)
8. Zhao Y Y, Liu Y J, Zheng S J, Huang M B, Meng L P. DFT study of the pentene radical cations: molecular and hyperfine structures. *Acta Phys-Chim Sin*, 2002, 18(12): 1081–1086 (in Chinese)
9. Zhang J L, Wang L B, Wu W P, Cao Z X. Electronic absorption spectra of linear cluster $\text{SC}_{2n}\text{S}^{2-}$ ($n=1-12$). *Acta Phys-Chim Sin*, 2004, 20(12): 1428–1433 (in Chinese)
10. Xia F, Lin Y Z, Xu Z X, Lin J D, Lü X, Liao D W. The theoretical computation on Ru_2N_2 cluster with C_{2v} symmetry. *Acta Phys-Chim Sin*, 2003, 19(12): 1119–1122 (in Chinese)
11. Zhang S Q, Wang Y Q, Zheng X M. Density functional theory investigation of the photoisomerization reaction of nitroalkanes and nitroaromatic compounds. *Acta Phys-Chim Sin*, 2006, 22(12): 1489–1494 (in Chinese)
12. Chen P Q, Sun H W, Li Z M, Wang J G, Ma Y, Lai C M. Density functional theory study on conformational conversion between crystal conformation and active conformation of herbicidal monosulfuron. *Acta Chim Sin*, 2006, 64(13): 1341–1348 (in Chinese)
13. Jin L X, Wang W L, Wu D B, Wang W N. Theoretical study on the structures and isomerization mechanisms of 5-methylcytosine- BH_3 complexes. *Acta Chim Sin*, 2007, 65(11): 1012–1018 (in Chinese)
14. Zhou Y D, Zeng H P, Jing H L, Yuan G Z, Ouyang X H. Synthesis and theoretical investigation of 5,7'-(iminomethyl)-bis-8-hydroxy-quinoline. *Chin J Org Chem*, 2006: 26(9): 1225–1231 (in Chinese)
15. Chen Z X, Xiao H M. Comparative investigation of the structure and IR of tetrazolate ion with density functional theory and MP2 Ab initio methods. *Chem J C U*, 1999,20(5): 782–787 (in Chinese)
16. Chen Z X, Xiao J M, Xiao H M, Chiu Y N. Studies on heat of formation for tetrazole derivatives with density functional theory B3LYP method. *J Phys Chem A*, 1999, 103: 8062–8066
17. Chen Z X, Xiao H M. Impact sensitivity and activation energy of pyrolysis for tetrazole compounds. *Int J Quantum Chem*, 2000, 79(6): 350–357
18. Chen Z X, Xiao H M, Yang S L. Theoretical investigation on the impact sensitivity of tetrazole derivatives and their metal salts. *Chem Phys*, 1999, 250(3): 243–248